

Spin Density Wave Instability for Chromium in Fe/Cr(100) Multilayers

J. Meersschant,¹ J. Dekoster,¹ R. Schad,² P. Beliën,² and M. Rots¹

¹*Instituut voor Kern- en Stralingsfysika, Celestijnenlaan 200D, B-3001 Leuven, Belgium*

²*Laboratorium voor Vaste Stof-Fysika en Magnetisme, Katholieke Universiteit Leuven, Celestijnenlaan 200D, B-3001 Leuven, Belgium*

(Received 21 April 1995)

Using perturbed angular correlation spectroscopy on Fe/Cr epitaxially grown multilayers, we observed an in-plane magnetization for Fe layers (thickness between 1.5 and 38 nm), while Cr (thickness between 7.5 and 40 nm) orders antiferromagnetically as a longitudinal (AF₂) spin density wave with the magnetization along the (100) direction normal to the layers, persisting well above the Néel temperature of bulk chromium. The Cr layers lose the Cr bulk magnetism and become paramagnetic, down to 4.2 K, or even nonmagnetic for thickness below 6.0 nm.

PACS numbers: 75.70.Fr, 75.50.Rr, 76.80.+y

The mechanism of the interlayer coupling in magnetic-nonmagnetic multilayers is a topic of intense research. The initial interpretation [1] of the experimental long-period oscillation (around 1.8 nm [2]) as a vernier effect between the spacer layer thickness and the theoretically short period deriving from a RKKY-type antiferromagnetic exchange coupling resolved the apparent conflict. Later on, indeed, a two-layer-period oscillation was observed on wedge-shaped Fe/Cr/Fe sandwiches with magneto-optical Kerr effect [3] and scanning electron microscopy with spin polarization analysis (SEMPA) [4]. Similar results were obtained on Cr overlayers on Fe by spin-polarized electron-energy-loss spectroscopy [5] and SEMPA measurements [6]. Calculations, however, indicate that the observed features of the spin polarization cannot merely be explained by RKKY-type exchange [7]. The contradicting results [8,9] on the net magnetization at the Cr(001) surface were interpreted [10] as a topological antiferromagnetism resulting from a high-index Cr surface or interface due to the wedge structure. One readily assumed here that the Cr spacer has the layered antiferromagnetic structure (AF₀) with (001) layers of alternating magnetization. Experiments do confirm the predicted magnetic moment enhancements at the surface of a Cr overlayer of Fe(100) but point out a drastic deviation from layered antiferromagnetic ordering within a few layers near the interface [11]. In this Letter we offer microscopic information on the magnetic behavior of Cr spacer layers in Fe/Cr(100) multilayers.

It is well known [12] that bulk Cr at the Néel temperature $T_N = 311$ K orders as an incommensurate spin density wave (I SDW) antiferromagnet with wave vector $Q_{SDW} = 0.958(2\pi/a)$ along the (100) direction, (a = lattice constant, Q is defined as the propagation vector of the SDW). The polarization changes from $S \perp Q$ in the transverse SDW phase (AF₁) above the spin-flip temperature ($T_{SF} = 123$ K) to $S \parallel Q$ in the longitudinal SDW phase (AF₂) below T_{SF} . In multilayers, however, there is no information on the stability of the SDW in thin Cr layers. Although the magnetism in thin Fe layers is well studied [13], the magnetic order in Cr thin films,

on the contrary, is still unknown. Yet it may be of crucial importance to understand the interlayer coupling in the Fe/Cr system. As pointed out by Unguris, Celotta, and Pierce [6], the observed alternating directions of magnetization at the Cr surface could be either due to an enhanced antiferromagnetism induced by the underlying Fe, or originating from the strong Fermi-surface nesting in paramagnetic Cr. To study the overall magnetic structure of Fe/Cr multilayers, one needs a direct determination of the net spin polarization *within* the Cr spacer, either induced by the interlayer coupling mechanism between two Fe layers or originating from the ground state SDW ordering. We use perturbed angular correlation spectroscopy (PAC) [14] to observe, at a radioactive (diamagnetic) trace impurity, the transferred hyperfine field originating from conduction electron polarization and thus derive the spatial distribution of magnetization.

Fe/Cr multilayers were grown on MgO by molecular beam epitaxy (MBE) techniques. Our samples were produced under exactly the same conditions as those on which the very high magnetoresistance effect was reported [15]. The quality of the multilayers was confirmed by *in situ* reflective high energy electron diffraction (RHEED) measurements. X-ray diffraction spectra showed peaks in the low angle range up to $2\theta = 10^\circ$ and clearly distinguishable satellite peaks in the high angle range around Fe/Cr(200). The multilayers with chromium thickness $0.6 \leq t_{Cr} \leq 5.1$ nm further showed the giant magnetoresistance effect with a maximum $\Delta\rho/\rho_s \approx 80\%$ and an oscillation period of 1.8 nm. Trace quantities of the nuclear ¹¹¹In(¹¹¹Cd) probe were incorporated into the layers by ion implantation at an energy of 80 keV up to doses around 10^{13} ions/cm². The estimated implantation profile has a projected range of 18 nm and a longitudinal straggling of 7 nm. High resolution time-differential (TD) PAC experiments on the γ - γ cascade of ¹¹¹Cd following the β^- decay of ¹¹¹In were performed, using a conventional fast-slow coincidence setup consisting of four BaF₂ detectors.

A PAC experiment is essentially the measurement of the exponential decay (coincidence spectrum) corresponding

to the lifetime of the intermediate nuclear state in the γ - γ cascade. An aligned nuclear subensemble in the intermediate state is *selected* simply by observing the preceding γ ray in a particular direction. The second (coincident) γ radiation is then emitted with a directional anisotropy. Because of the hyperfine interaction the nuclear alignment reorients under the influence of the hyperfine fields and the anisotropy becomes time dependent, reflecting the ‘‘Larmor precession.’’ The measured frequency ν is proportional to the hyperfine field by a factor 2.33 MHz/T. Four detectors, encompassing 90° with each other (Fig. 1), are used to measure γ - γ coincidences. With the mutual coincidence spectra one constructs the anisotropy ratio $R(t)$ (so-called PAC time spectrum [14]). The experimental precession pattern thus obtained is then compared to well-known theoretical curves to yield the magnitude and orientation of the hyperfine fields, and their absolute fractions. In case of a ferromagnetic or a layered antiferromagnetic (AF₀) ordering, described assuming a Lorentzian distribution in the hyperfine field characterized by mean value ν and width $\delta\nu$, one uses

$$R(t) = a_0 + \sum a_n e^{-n\delta\nu t} \cos(n\nu t), \quad n = 1 \text{ and/or } 2, \quad (1)$$

to fit the anisotropy function. In case of an incommensurate SDW antiferromagnetic ordering (AF₁ or AF₂), one needs to account for the Overhauser distribution in the hyperfine field [16] and the anisotropy function is described by

$$R(t) = a_0 + \sum a_n J_0(n\nu t), \quad n = 1 \text{ and/or } 2, \quad (2)$$

with $J_0(n\nu t)$ the Bessel function of zeroth order.

One should realize that, in a PAC experiment, the spin alignment in the intermediate state is axially symmetric with respect to the emission direction of the first γ ray. In a naive picture, one can understand that the initial spin alignment is restored twice per hyperfine interaction period when the hyperfine field is perpendicular to the detector plane but only once when the hyperfine field is in plane under 45° with the detectors. We can, therefore, deduce the orientation of the magnetization by comparing the amplitude ratio of the two harmonics in different geometries. After demagnetizing the sample at room temperature, data were subsequently obtained in two geometries by simply turning the sample normal [the (100) direction] either perpendicular or in plane relative to the detectors. In the first geometry [Fig. 1(a), so-called perpendicular geometry] the (010) and (001) crystal directions point in between the detectors, while in the second configuration [Fig. 1(b), in-plane geometry] these directions were pointing 45° out of the detector plane. To illustrate our data analysis and interpretation we first show the PAC time spectra taken on a 38 nm thick Fe film and a 40 nm thick Cr film.

The PAC time spectra taken at 289 K on a 38 nm thick Fe film (Fig. 2) display the well-known [17] hyperfine interaction frequency $\nu = 89.0(2)$ MHz with distribution

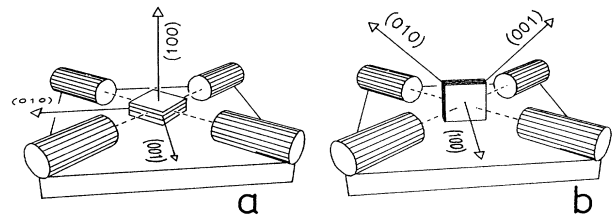


FIG. 1. Schematic view of the configuration of the detectors and the sample (a) in the perpendicular geometry and (b) in the in-plane geometry used in the PAC experiments.

$\delta\nu = 1.1(1)$ MHz, Eq. (1), indicating that the Cd probes take a regular substitutional position in the Fe lattice. In the perpendicular geometry the precession pattern reflects the single frequency ν [Fig. 2(a)], while the in-plane geometry leads to a superposition of the single and the double frequency [Fig. 2(b)]. This observation immediately fixes the orientation of the Fe hyperfine field, and thus the magnetization, along the two equivalent in-plane (001) directions.

In the 40 nm thick Cr layer measured at 77 K (Fig. 2) we observe the hyperfine interaction with a distribution of the Overhauser type. The data are well reproduced by Eq. (2), meaning that the incommensurate SDW magnetic order is the appropriate approach. In the perpendicular and in-plane geometry we observe the double and the single frequency, respectively [see Fig. 2(c) and 2(d)]. This clearly proves that the Cr hyperfine field is oriented along the (100) direction *normal to the layers*. In addition, the Néel temperature was shifted upwards ($T_N > 533$ K) and the magnetic hyperfine field notably enhanced as compared to the Cr bulk values. For instance, the value measured at room temperature almost exactly corresponds to the value below the spin-flip temperature in bulk polycrys-

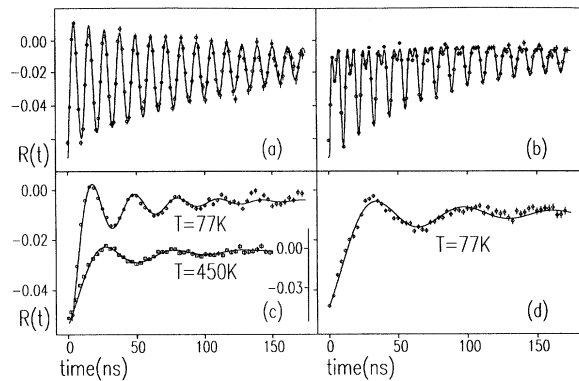


FIG. 2. The reference PAC time spectra for a 38 nm Fe film, grown on MgO, taken at 289 K, (a) perpendicular and (b) in-plane geometry. The solid lines are theoretical fits using Eq. (1). The PAC time spectra for a MgO/2 nm Fe/40 nm Cr film taken in the perpendicular (c), and in-plane (d) geometry. The solid line corresponds to an incommensurate SDW, Eq. (2), of maximum interaction frequency $\nu = 15.8(2)$ MHz for the spectra taken at 77 K and $\nu = 10.0(2)$ MHz at $T = 450$ K.

talline chromium [18]. The observed interaction frequency gradually decreases at higher temperatures [Fig. 2(c)], but a definite magnetic spectrum was measured until the resistivity anomaly had totally disappeared [19]. The orientational anisotropy of the hyperfine field as well as the enhancement of the Néel temperature inhere in strained chromium [12].

Both the Fe and Cr experiments indicate a large majority of probes ending up in the substitutional lattice position. The spectra obtained on Fe/Cr multilayers, therefore, are expected to reflect the following atomic configurations for the implanted ^{111}Cd probes: The nuclear probe is located either in an iron or a chromium environment, but possibly also at the interface. The latter signal is unknown, yet we expect that shifted frequencies with a broad distribution contribute, together with probes in ill-defined environments, to the drastic loss of anisotropy within a rather short time interval.

As an example of the measurements on the multilayered structures $\text{MgO}/(t_{\text{Cr}}\text{Cr}, t_{\text{Fe}}\text{Fe})_8$, we show in Figs. 3(a) and 3(b) the PAC time spectra measured at 289 K for the case $t_{\text{Cr}} = 7.5$ nm and $t_{\text{Fe}} = 2.0$ nm. In the multilayers the magnetization is oriented precisely as in the thicker single layers. In Fe layers with a thickness between 1.5 and 30 nm the hyperfine field is oriented *in plane* along the (001) directions, while in the Cr layers with a thickness between 6 and 40 nm the hyperfine field is oriented *out of plane* along the (100) direction. This means that in Fe/Cr(100) multilayers the magnetization in the Cr layer is oriented *perpendicular* to the Fe magnetization. Resistivity measurements located the magnetic transition in the Cr layers of the present multilayer at $T_N = 525(5)$ K. The resistivity anomaly at T_N of the multilayers was smeared out as previously perceived with strained chromium [19]. The PAC spectra obtained at 533 K are shown in Figs. 3(c) and 3(d). As the Curie point of Fe (at 1043 K) has not yet been reached, the Fe signal is still present, but the spectra are clearly taken above the chromium Néel temperature. Indeed, the Cr contribution that is explicitly shown consists of a rather slow decay. We interpret this fraction to be due to probes in paramagnetic bcc chromium with small electric field gradients that are the result of strain in the multilayer. Subsequent measurements at room temperature reveal *exactly* the same “magnetic” spectra as prior to heating.

The PAC time spectra for $t_{\text{Fe}} = 3.0$ nm and $t_{\text{Cr}} = 0.9$ nm, 3.3 nm, and 5.1 nm are shown in Fig. 4. We repeatedly observe as a function of Cr-layer thickness essentially the same spectrum, different only in the relative amount of both the Fe contribution and a slowly varying background. The latter contribution to the spectra is reminiscent of the chromium contribution in the spectra taken on thicker Cr layers above the Néel temperature (Fig. 3). For this reason we claim the presence of paramagnetic chromium but strained bcc due to the lattice mismatch in the epitaxial growth. Remarkably, the Cr

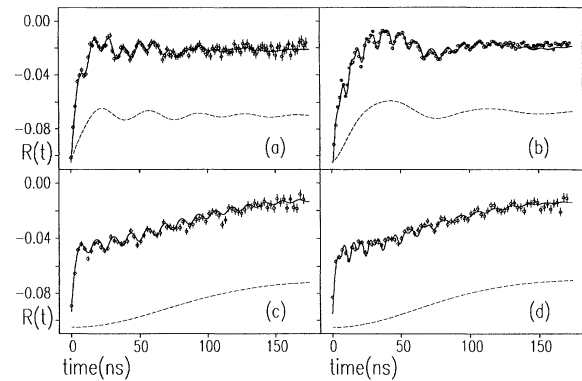


FIG. 3. (a),(b) The PAC time spectra for a multilayer $\text{MgO}/(2.0 \text{ nm Fe}/7.5 \text{ nm Cr})_8$ at 289 K. The solid line is a fitted curve using both Eqs. (1) and (2). The PAC time spectra measured at 533 K [(c) and (d)] are fitted by a composite of Eq. (1) and an exponential function. The spectra on the left are obtained in the perpendicular geometry while the spectra on the right-hand side are measured with the sample in the in-plane geometry. The dashed lines visualize the chromium contribution.

layers with $t_{\text{Cr}} \leq 5$ nm were probed here as paramagnetic down to 4.2 K or even nonmagnetic, thus excluding also antiferromagnetic ordering in ferromagnetic sheets.

Size effects were recently reported on nanocrystalline chromium by neutron diffraction techniques [20,21]. When magnetically ordered, the grains never reflected the transversely polarized AF_1 SDW phase; rather the AF_0 (or AF_2) phase was present. In our experiments on thin Cr films the incommensurate structure best fits the

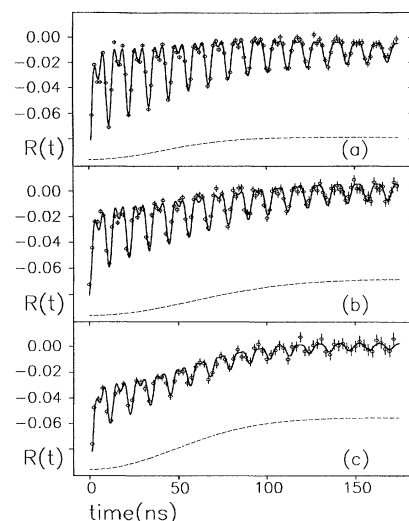


FIG. 4. PAC time spectra taken on $\text{MgO}/[\text{Fe}(3.0 \text{ nm})/\text{Cr}(t_{\text{Cr}})]_{10}$ multilayers with Cr thickness up to 5.1 nm, obtained at 293 K in the in-plane geometry. The Cr thicknesses are (a) 0.9 nm, (b) 3.3 nm, and (c) 5.1 nm. The dashed lines represent the chromium contribution.

data and the AF₂ SDW phase is evidenced on the basis of the hyperfine field magnitude yet more explicitly by its orientation. In addition, the presence of a transversal SDW eventually induced by the underlying Fe could be refuted by measuring the same antiferromagnetic order in MgO/40 nm Cr as well as in MgO/2 nm Fe/40 nm Cr/2 nm Fe. Apparently a single-*Q* type of ordering is sustained up to epitaxially grown thickness of at least 40 nm. This observation correlates well with the experience [12] that a single-*Q* wave can be induced also by stress or field cooling. We thus conclude that, in thin Cr(100) layers, chromium orders as a *longitudinally* polarized spin density wave structure, with the spins along a single *Q* vector oriented parallel to the growth direction of the multilayers.

Already two decades ago Schmidt *et al.* [22] reported the observation of superconductivity, yet no detectable antiferromagnetic ordering, in ion beam sputtered chromium films of estimated average grain size around 12 nm. Magnetization measurements [23] on ultrafine bcc Cr particles with approximate diameter of 2 nm reveal that the particles are paramagnetic down to 4.2 K. In neutron-diffraction measurements on powdered or granular chromium samples, the antiferromagnetic order was not observed when the grain size was less than 16 nm [21]. The present experiments show the existence of a rather abrupt threshold below 6 nm for the crossover from the magnetic to paramagnetic state in chromium layers. The suppression of the antiferromagnetic order below a critical layer thickness is correlated with the type of SDW structure (AF₂) and its wavelength, being of the order of 6 nm in bulk chromium [12]. Therefore, the oscillatory exchange coupling in the Fe/Cr system [2–6] should not be related to the ground state antiferromagnetic order in the Cr spacer. Rather the total decoupling as observed for Cr spacer layers with a thickness larger than 5.0 nm [24] should be considered to be caused by the onset of the SDW antiferromagnetic order inside the Cr spacer.

In conclusion, we used PAC spectroscopy to determine the magnetic state of epitaxially grown Fe/Cr(100) multilayers. We demonstrated that in the Fe layers the magnetization lies along the two (100) axes in plane. A longitudinal spin-density-wave antiferromagnetic order (AF₂) with *Q* vector perpendicular to the layers readily explains the perpendicular magnetization in the chromium layers, at least up to a thickness of 40 nm. A potentially interesting experiment could be to confirm this conclusion by neutron diffraction. We noticed that the ordering temperature in the Cr layers depends on the thickness and reported that the antiferromagnetic ordering in layered chromium is suppressed below a thickness of 6 nm. This observation for the first time clearly provides evidence for the collapse of the spin density wave in epitaxial Cr layers when the thickness of the Cr film approaches the spin modulation period. Therefore, we have proven that (SDW) antiferromagnetic ordering in chromium is not the

dominant mechanism responsible for the indirect coupling in the Fe/Cr system.

The authors thank S. M. Dubiel for helpful discussions and comments. We benefited greatly from the analysis program by the courtesy of N. P. Barradas (CFNUL at Lisbon, Portugal). The work at the K. U. Leuven was made possible by the support of the Belgian Concerted Action (GOA), the Interuniversity Attraction Poles (UIAP), and the Interuniversity Institute for Nuclear Science (IIKW). J.M. was supported by the IWT foundation Contract No. 943054.

-
- [1] P. Bruno and C. Chappert, Phys. Rev. B **46**, 261 (1992).
 - [2] S. S. P. Parkin, N. More, and K. P. Roche, Phys. Rev. Lett. **64**, 2304 (1990).
 - [3] S. T. Purcell, W. Folkerts, M. T. Johnson, N. W. E. McGee, K. Jaeger, J. aan de Stegge, W. B. Zeper, W. Hoving, and P. Grünberg, Phys. Rev. Lett. **67**, 903 (1991).
 - [4] J. Unguris, R. J. Celotta, and D. T. Pierce, Phys. Rev. Lett. **67**, 140 (1991).
 - [5] T. G. Walker, A. W. Pang, H. Hopster, and S. F. Alvarado, Phys. Rev. Lett. **69**, 1121 (1992).
 - [6] J. Unguris, R. J. Celotta, and D. T. Pierce, Phys. Rev. Lett. **69**, 1125 (1992).
 - [7] Z.-P. Shi, P. M. Levy, and J. L. Fry, Phys. Rev. Lett. **69**, 3678 (1992).
 - [8] C. Carbone and S. F. Alvarado, Phys. Rev. B **36**, 2433 (1987).
 - [9] L. E. Klebanoff, S. W. Robey, G. Liu, and D. A. Shirley, Phys. Rev. B **30**, 1048 (1984).
 - [10] A. Vega, L. C. Balbas, A. Chourairi, C. Demangeat, and H. Dreysse, Phys. Rev. B **49**, 12797 (1994).
 - [11] C. Turtur and G. Bayreuther, Phys. Rev. Lett. **72**, 1557 (1994).
 - [12] E. Fawcett, Rev. Mod. Phys. **60**, 209 (1988).
 - [13] M. Przybylski, J. Korecki, and U. Gradmann, Hyperfine Interact. **57**, 2053 (1990).
 - [14] For an excellent introduction to PAC, see Th. Wichert and E. Recknagel, in *Microscopic Methods in Metals*, edited by U. Gonser (Springer, Berlin, 1986), p. 317.
 - [15] R. Schad, C. D. Potter, P. Beliën, G. Verbanck, V. V. Moshchalkov, and Y. Bruynseraede, Appl. Phys. Lett. **64**, 3500 (1994).
 - [16] H. C. Binski, Phys. Lett. **42A**, 295 (1972).
 - [17] G. N. Rao, Hyperfine Interact. **7**, 141 (1979).
 - [18] R. Venegas, P. Peretto, G. N. Rao, and L. Trabut, Phys. Rev. B **21**, 3851 (1980).
 - [19] J. Mattson, B. Brumitt, M. B. Brodsky, and J. B. Ketterson, J. Appl. Phys. **67**, 4889 (1990).
 - [20] Y. Tsunoda, H. Nakano, and S. Matsuo, J. Phys. Condens. Matter **5**, L29 (1993).
 - [21] M. R. Fitzsimmons, J. A. Eastman, R. B. Von Dreele, and L. J. Thompson, Phys. Rev. B **50**, 5600 (1994).
 - [22] P. H. Schmidt, R. N. Castellano, H. Barz, B. T. Matthias, J. G. Huber, and W. A. Fertig, Phys. Lett. **41A**, 367 (1972).
 - [23] T. Furubayashi and I. Nakatani, J. Appl. Phys. **73**, 6412 (1993).
 - [24] M. Donath, D. Scholl, D. Mauri, and E. Kay, Phys. Rev. B **43**, 13164 (1991).